Chalcogenide Letters Vol. 10, No. 9, September 2013, p. 341 - 348

A NUMERICAL SIMULATION ON ZINC SULFIDE (ZnS) BUFFER LAYER IN $CuInS_2$ BASED THIN FILM SOLAR CELL

HADIBAH RAMLI[a*], SHARUL KAMAL ABDUL RAHIM[a],
THAREK ABD RAHMAN[a], MUHAMMAD MUHAIMIN AMINUDDIN[b]
[a]*Wireless Communication Center, Universiti Teknologi Malaysia, Skudai, 81310, Johor Bharu, Johor Darul Ta'zim, Malaysia*
[b]*IC MICROSYSTEMS Sdn. Bhd., Unit B-G-03, SME Technopreneur Centre 2, 2260, Jalan Usahawan 1, 63000 Cyberjaya, Selangor Darul Ehsan, Malaysia.*

Zinc sulfide (ZnS) is the most suitable candidates for the $CuInS_2$ among of the corresponding alternatives buffer layer. In this paper, the simulated performance of the baseline model of conventional CdS buffered-$CuInS_2$ based thin film solar cell is proven with the performance of fabricated model. This method of simulation uses the experimental data from literature and an adequate fitting procedure. Meanwhile, the effect of the ZnS and the widths of buffer layer (CdS and ZnS) with the focus on energy diagram have been investigated.

(Received August 9, 2013; Accepted September 23, 2013

Keywords: Copper Indium Sulfide, Zinc Sulfide, Cadmium Sulfide, Buffer layer

1. Introduction

Generally, achieving the high efficient Cd-free buffer in thin film solar cell in comparison with those obtained for the solar cell with CdS buffer layer is an important milestone of this thin film solar cell technology. The role of buffer layer is to minimize the interface recombination and provide as large band bending across the junction as possible [4]. The device efficiency η for the up to 20.3% for Cu(In,Ga)Se [1] and around 11% for the $CuInS_2$ [2-3] has been demonstrated with well conducting of CdS buffer layer. However, the environmental issues and toxicity contamination of CdS have become major objectives for the development of a Cd-free in thin film solar cell field. Furthermore, the low energy band gap of CdS (~2.4 eV) leads to higher absorption in shorter wavelength of the incoming solar irradiation.

Due to this, ZnS is considered one of the best materials for the $CuInS_2$ among other alternatives buffer layer. In comparison with CdS, the ability of ZnS provides a good lattice matching to $CuInS_2$ absorber layer as well as has higher energy bandgap (~3.5 eV) and high refractive index, which increase the photon absorption in absorber layer [5-7]. This is also included with its non-toxic material and environmentally safe and thus, the issue of Cd-free buffer layer for Cu-chalcopyrite thin film solar cells can be achieved. In this work, the baseline model of CdS buffered of $CuInS_2$ (ZnO:Al/i-ZnO/buffer/$CuInS_2$/Mo/glass) based thin film solar cell from [2] is simulated using Silvaco TCAD.

Apart from that, the CdS buffer layer is replaced by ZnS buffer for baseline cell $CuInS_2$ based thin film solar and device performance is compare by current-voltage (j-V characteristics) and external quantum efficiency (EQE). In this simulation, the widths for CdS and ZnS buffer layer are investigate to show the effect of energy diagram at 0 V and 0.6 V (from *j-V* curves) towards of properties of solar cell.

* Corresponding email: hadibahramli@yahoo.com

2. Simulation details

The baseline model based on solar cell with ZnO:Al/i-ZnO/CdS/$CuInS_2$/Mo/glass are chosen from previous research work. The input parameters for this baseline model are taken out from available experimental data on solar cell to yield the solar cell parameter values are closest to the reported in [2].

For the device simulation using two dimensional Silvaco TCAD program, the following layer are applied by stack sequence: 2 μm thick $CuInS_2$ absorber layer followed by a 50 nm thick CdS buffer and a 100 nm thick i-ZnO layer with 400 nm thick ZnO:Al of window bilayer. The 500 nm thick of Al and Mo are served as front and back contact as shown in Figure 1. The value of thicknesses are taken out from [2-3] and [8]. The interface recombination between $CuInS_2$ absorber layer and CdS buffer layer is assumed of 10^6 cm s^{-1} for electrons and as well for holes.

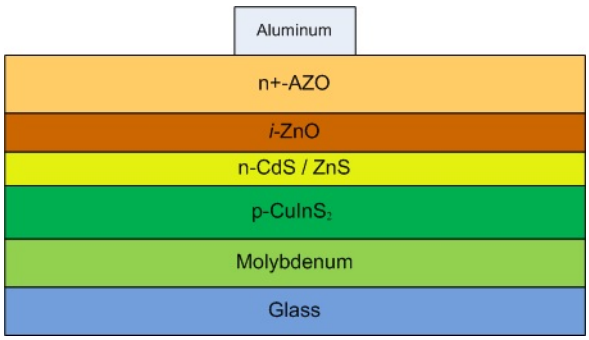

Fig. 1. Schematic model of absorber layer with CdS or ZnS buffer layer used in TCAD simulation.

Table I. The physical parameters applied in modeling of solar cells devices consisting of band gap energy E_g, electron affinity χ, relative permittivity ε_r, effective density of states in conduction N_c and valence band N_v and electron mobilities of electrons μ_e and holes μ_h.

	$CuInS_2$	CdS	ZnS	i-ZnO	AZO
E_g (eV)	1.55	2.5	3.7	3.4	3.5
χ(eV)	4.06	4.27	4.27	4.4	4.4
ε_r	9.76	11.9	8.46	9	9
N_c ($1/cm^3$)	1.6×10^{18}	1.63×10^{18}	2.46×10^{18}	2.9×10^{18}	2.9×10^{18}
N_v ($1/cm^3$)	3.71×10^{19}	7.56×10^{19}	3.14×10^{19}	2.79×10^{20}	2.79×10^{20}
μ_e (cm^2 V^{-1} s^{-1})	1×10^{-9}	5.5×10^{-13}	5.5×10^{-13}	5.5×10^{-13}	1×10^{-10}
μ_h (cm^2 V^{-1} s^{-1})	1×10^{-9}	5.5×10^{-13}	5.5×10^{-13}	5.5×10^{-13}	1×10^{-10}

Other layer properties of model are presented in Table I. These parameters values are discussed in [9-13]. The parameters given above and in Table I are applied in modeling of baseline solar cells.

In addition to the base line model, the solar cell with ZnS buffer layer is replaced as comparable for CdS buffer layer. The *j*-V characteristics and EQE simulation results are performed under standard condition at air mass (AM) 1.5.

3. Results

3.1 Base line model with CdS and ZnS buffer layer

Figure 2 displays the simulated *j-V* curve of ZnO:Al/i-ZnO/CdS/$CuInS_2$/Mo/glass baseline model thin film solar cell and solar cell with ZnS buffer layer . The solar cell efficiency η, short circuit density current J_{sc}, open circuit voltage V_{oc} and fill factor *FF* values obtained from the simulation are then used as for comparing with fabricated $CuInS_2$ baseline model thin film solar cell by [2], are given in Table II.

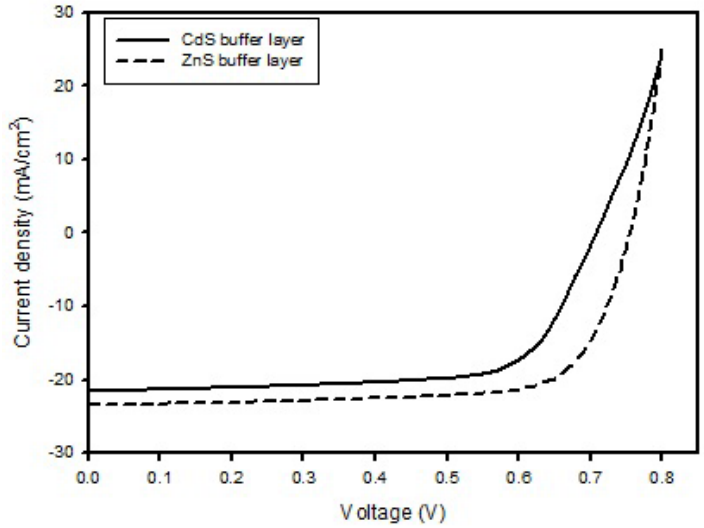

Fig. 2. Simulated light j-V curve of a ZnO:Al/i-ZnO/CdS/$CuInS_2$/Mo/glass thin film and ZnO:Al/i-ZnO/ZnS/$CuInS_2$/Mo/glass thin film solar cell from baseline model.

As it can be seen in Figure 2 and Table II, the simulated CdS buffer based $CuInS_2$ baseline cell shows a comparable performance as corresponding to the fabricated device with CdS buffer thin film baseline cell. In comparison to the simulated CdS buffer based $CuInS_2$ baseline cell, the short-circuit current density J_{sc} of simulated baseline model with ZnS buffer cell shows the increment of about 2.0 mA/cm^2. In addition, the cell with ZnS buffer layer gives an enhancement of V_{oc} of 0.795 V, fill factor *FF* of about 73.6% and efficiency η is 13.8%. As the improvement J_{sc} from simulated $CuInS_2$ thin film solar cell, it is obviously shows that $CuInS_2$ solar cell with ZnS buffer benefits from its increased window transparency [2] in the blue response (wavelength at 350 nm-500 nm) compared to the solar cell with CdS buffer layer. This is also supported by the external quantum efficiency simulations of corresponding of solar cells with ZnS and CdS buffer, which are shown in Fig. 3.

It is clearly shown that the ZnS buffer layer has higher transparency in the blue response region in comparison to the CdS layer. Figure 3 shows the corresponding EQE curves for the performance of solar cells simulated in Figure 1. The EQE with CdS buffer layer is lower than with respect to the ZnS buffer layer in the wavelength regime of 350nm-900nm. The steeper slope for shorter wavelength between 400 nm and 500 nm is occurred in CdS buffer of 20% and exhibit a higher response of 67% at the wavelengths larger than 800 nm. Whereas, the solar cell with ZnS buffer shows the increasing spectral response 78% from the wavelength 350 nm to 900 nm. This is probably due to the applied of small surface recombination rate at the interface (between ZnS and $CuInS_2$) S_p of ≈10^6 cm/s in simulation model and thus, leading to the increasing of open circuit voltage V_{oc} and the short current density J_{sc}.

Table 2. Comparison of the performance of ZnO:Al/i-ZnO/buffer/$CuInS_2$/Mo/glass thin film solar cell

$CuInS_2$ solar cell	Jsc (mA/cm^2)	Voc (V)	FF (%)	η (%)
Baseline cell by [Ennoui]	21.4	0.708	68.1	10.3
Simulation with CdS buffer	21.5	0.707	69.6	10.7
Simulation with ZnS buffer	23.5	0.795	73.6	13.8

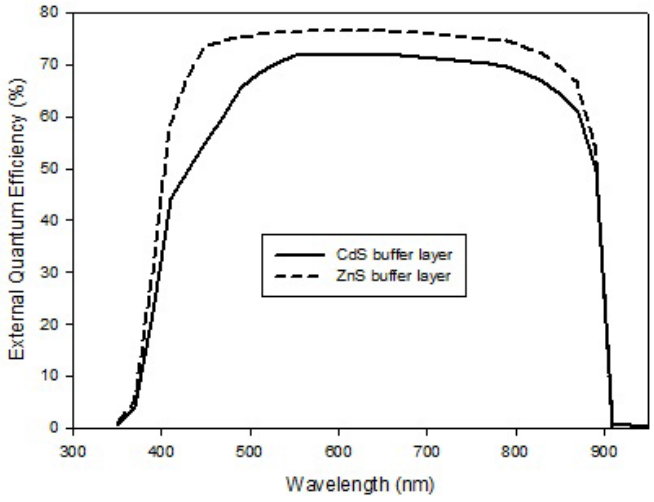

Fig. 3. External Quantum Efficiency of CuInS2 baseline cell with CdS and ZnS buffer layer, respectively.

3.2 Effect of various widths of CdS and ZnS layer

Figure 4 shows a comparison of the simulated widths of CdS and ZnS buffer layer (also see Figure 5). In this simulation, the widths of CdS and ZnS buffer are varied from 50 nm to 70 nm. As the width of CdS buffer layer is increase, the J_{sc} is declined due to the larger photon losses [15]. It can be seen in Figure 4 clearly, the reducing trends in J_{sc} as the buffer layer width increases for the CdS buffer layer. This is supported that more numbers of photon will be absorbed by the CdS buffer layer and thus, reduces J_{sc}. The width of 50 nm CdS buffer layer gives the highest J_{sc} for this simulated $CuInS_2$/CdS buffer layer as shown in Table III. It is clearly shows that thinner buffer layer would produce majority photons to pass through the buffer layer without being absorbed [16]. However, the J_{sc} remaining constantly as the width of ZnS buffer layer increases from 50 nm to 70 nm.

This is due to the numbers of photons are passing through the ZnS buffer region and being absorbed in absorber region. The V_{oc} of the solar cell increases with the width of CdS and ZnS buffer layer as shown in Figure 4, Table III and Table IV.

Meanwhile, the *FF* and device efficiency has shown reducing trends as the widths are increased for the CdS buffer. As the buffer layer increased to 70 nm, the *FF* and efficiency rapidly dropped. This is due to the photon loss occurred in CdS buffer layer. Less number of photons are generated, it would generates less number of photons are absorbed in absorber layer and hence less power are generated by solar cell. However, the *FF* is slightly increasing with the width of ZnS buffer layer and efficiency of the device remained constant at 13.8% as depicted in Figure 4. Again, it is related to the number of photons is not being absorbed in the ZnS buffer layer due to the higher transparency [2].

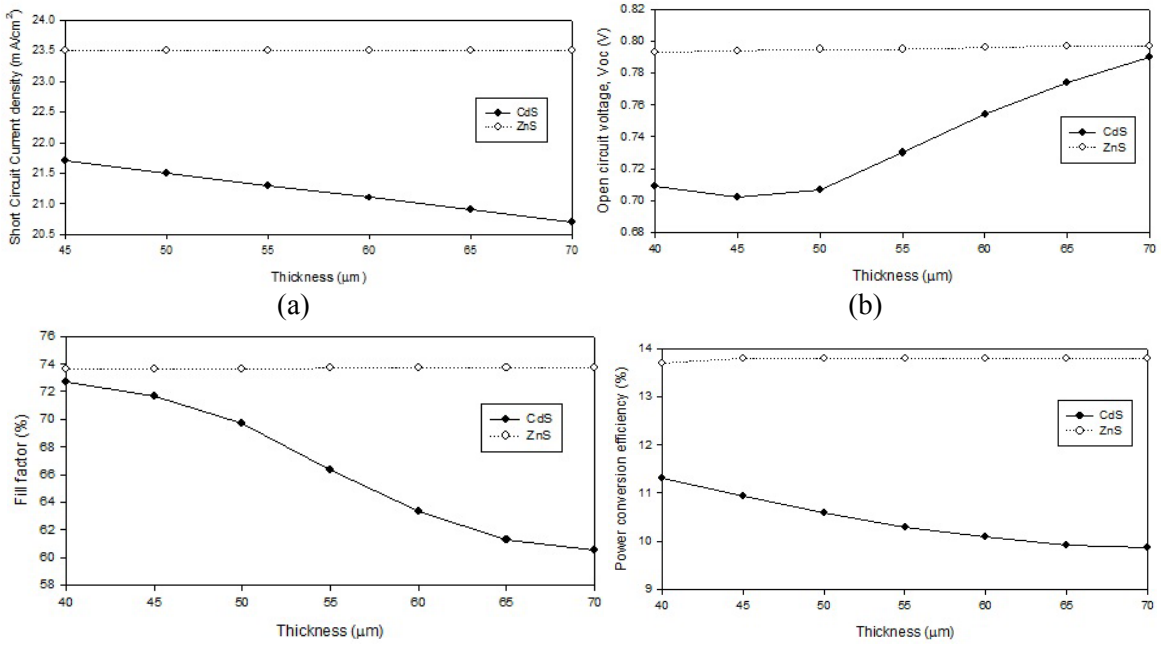

Fig. 4. Effect of CdS and ZnS width buffer layer in $CuInS_2$

Table 3. Performance of $CuInS_2$ based thin film solar cell with CdS buffer layer

CdS width layer, W_1(nm)	J_{sc} (mA/cm^2)	V_{oc} (V)	*FF* (%)	η (%)
50	21.5	0.707	69.7	10.6
55	21.3	0.730	66.3	10.3
60	21.1	0.753	63.3	10.1
65	20.9	0.774	61.3	9.91
70	20.7	0.790	60.5	9.87

Table 4. Performance of $CuInS_2$ based thin film solar cell with ZnS buffer layer

ZnS width layer, W_2 (nm)	J_{sc} (mA/cm^2)	V_{oc} (V)	*FF* (%)	η (%)
50	23.5	0.795	73.6	13.8
55	23.5	0.795	73.7	13.8
60	23.5	0.796	73.7	13.8
65	23.5	0.797	73.7	13.8
70	23.5	0.797	73.7	13.8

Fig. 5 is depicted the simulated EQE for CdS and ZnS buffer layer as the width is varied. The simulated EQE curve is shifted downward with the increasing width of CdS buffer layer. At shorter wavelength, the absorption of photon are will be less in ZnS buffer layer due to energy bandgap of CdS is lower than the bandgap of ZnS.

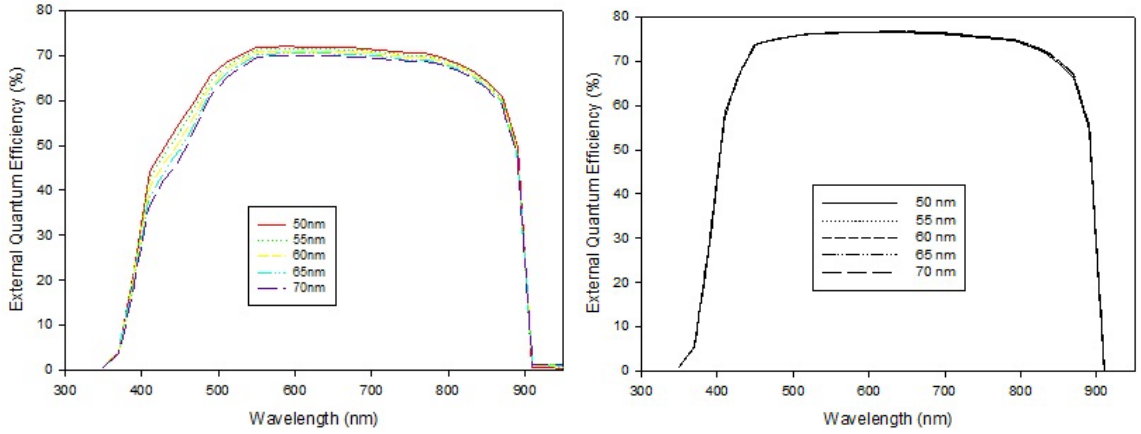

(a) (b)

Fig. 6. Simulated of spectral response with different widths of (a) CdS and (b) ZnS buffer layer

3.3 Energy band diagram in $CdS/CuInS_2$ and $ZnS/CuInS_2$ interface region

The simulated j-V characteristics for four widths CdS and ZnS buffer layer between 50 nm and 70 nm at point 0 V and +0.6 V as indicated are shown in Figure 6. Thus, the graph simulated energy diagrams of the CdS/CuInS2 and ZnS/CuInS2 interface region equal to 50 nm and 70 nm at 0 V (see Figure 7 (a), (b)) and +0.6 V (see Figure 9 (a), (b)) which the losses of J_{sc} and *FF* in $CdS/CuInS_2$ interface can be understood from the simulated energy diagram.

It is clearly shown that in this model, as the extension of CdS buffer layer results the reduction of collection of photo-generated carrier at 0.6 V as shown in Figure 7(a). For the ZnS buffer layer, there are no changes for the current collection at both 50 nm and 70 nm as depicted in Figure 7 (b) and Figure 8 (b). As the comparison at 0 V and 0.6 V, the number of photon is not gives affected in ZnS buffer. This is due to the less numbers of photon loss occurred at the point forward biases (0 V and 0.6 V) in ZnS buffer layer.

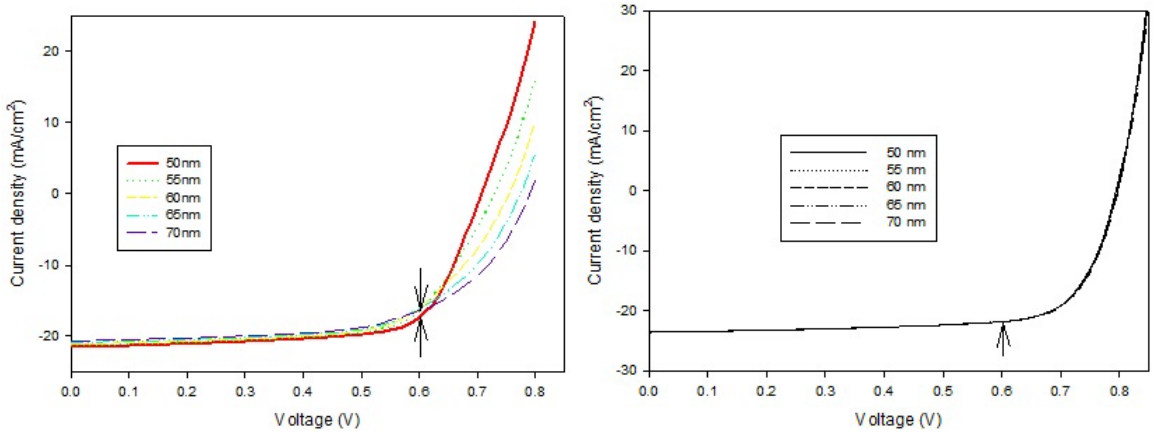

(a) (b)

Fig. 6. Simulated light j-V characteristics with different widths of (a) CdS and (b) ZnS buffer layer

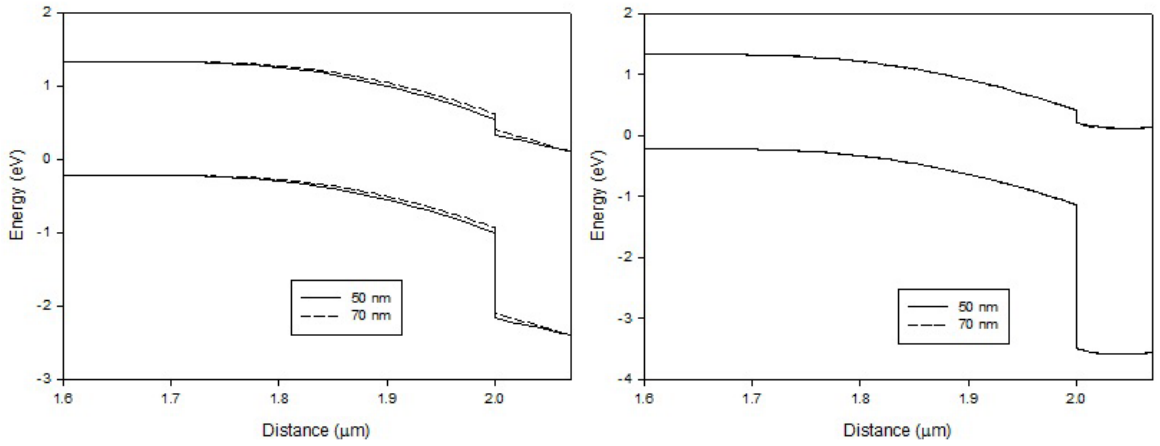

Fig. 7. Simulated band diagram at 0 V corresponding to 50 nm (solid line) and 70 nm (dashed line) widths of the (a) CdS (b) ZnS buffer layer

As seen from simulated energy diagram in Figure 8 (b), the decreasing of J_{sc} and *FF* is related to the absorption of more photon energy in CdS buffer layer accordance to the simulated *j-V* characteristics in Figure 5 and Table III (in CdS buffer layer). Thus, the photo-generated collection is reducing in absorber layer [4] as shown Figure 8 (a). Another factor that lead to reduced of current collection with the increasing width in CdS buffer is smaller driving force for holes generated in the CdS. This is supported by [3] that the less driving forces, the more holes recombine in CdS layer before they are emitted in $CuInS_2$ absorber layer.

Meanwhile, the simulated energy band diagram result for the ZnS buffer layer is in accordance to the simulated j-V characteristics. At 0 V, the simulated energy diagram shows no reduction in current collection. Also, in 0.6 V, the graph gives the same results as in 0 V energy diagram as shown in Figure 7 (b) and Figure 8 (b). Thus, the open circuit current density J_{sc} is constantly at 23.5 mA/cm^2 and fill factor *FF* shows the increasing trends as the expansion in width of ZnS buffer. This is strongly relates to the performance of external quantum efficiency which the less absorption of photon occurred in ZnS buffer layer due to high bandgap (3.5 eV).

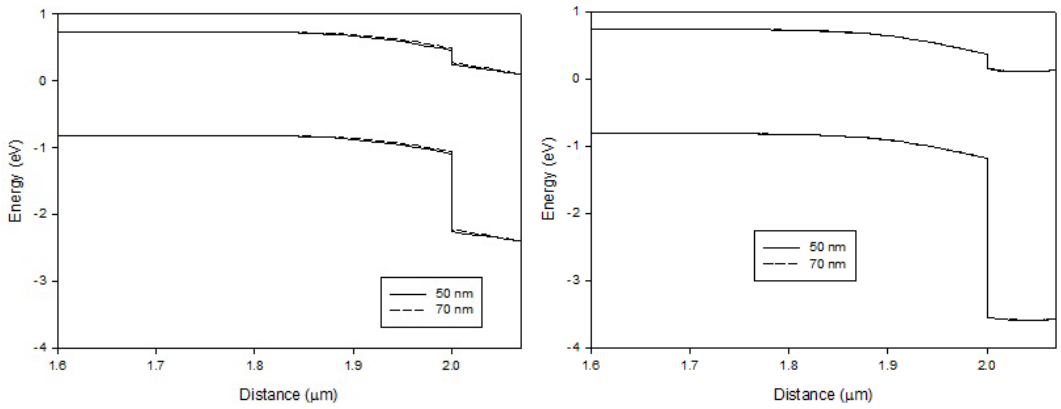

Fig. 8 Simulated band diagram at 0.6 V corresponding to 50 nm (solid line) and 70 nm (dashed line) widths of the (a) CdS (b) ZnS buffer layer.

4. Conclusion

The base line model of CdS buffer-$CuInS_2$ based solar cell has been established in this simulation. Similarly, the simulated of performance of this baseline model is in good comparison with fabricated baseline model. In this simulation, it is found that the $CuInS_2$ solar cell with ZnS buffer layer is suitable as Cd-free candidate for buffer layer. The device efficiency is improved as well as with short current density J_{sc}, open circuit current V_{oc} and fill factor *FF*. The electrical properties energy diagram in CdS and ZnS buffer layer has been investigated in terms of width of buffer layer. It is shows a good agreement that the more absorption of photon occurred in CdS buffer layer compared to ZnS buffer layer. This is also supported by finding that short circuit current density J_{sc}, fill factor *FF* and efficiency shows a decreasing trends with widths of CdS buffer layer increases. Meanwhile, the expand widths of ZnS gives constantly values for the short circuit current density J_{sc}. The changes of electrical properties of ZnS buffer layer is caused by the less absorption of photon and current collection in buffer region.

Further investigation on simulation of absorber layer widths and effect on electron to hole concentration in absorber layer are key issues for more understanding of ZnS/$CuInS_2$ hetero-structure in thin film solar cell in future research.

Acknowledgements

This work is funded by the National Flagship Research University (RU) Grant funded by the Ministry of Science, Technology and Innovation (MOSTI) (Q.J130000.2423.00G35). The authors acknowledge the ICMicrosystem Sdn. Bhd. for providing the technology support and fruitful discussion in this solar cell project.

References

[1] P. Jackson, D. Hariskos, E. Lotter et al., Progress in Photovoltaics: Research and Applications, **19**(7), 894 (2011).
[2] Ennaoui A, M Bar Highly-efficienct Cd-free CuInS2 Thin Film Solar Cells and Mini-Modules with Zn(S,O) Buffer Layers Prepared by An Alternative Chemical Bath Process
[3] S. S. Schmidt, D. Abou-Ras, T. Unold, T. Eisenbarth, H. Wilhelm et al, J. App. Phy., **110**, 0645151 (2011).
[4] B. Alessio, R. Alessandro, Nova Science Publishers Inc, pp.128-131, 2011.
[5] L. Zhou, Y. Xue, L.I. Jianfeng, Journal of Environmental Scienes, **21**, 76 (2009).
[6] Y. Z. Zhao, S. C. Eou, J. K. Sang, Materials Chemistry and Physics, **135**, 287 (2012).
[7] D. Y. Hwang, J. H. Ahn, Nanoscale Research Letter, vol. 2012.
[8] S. W. Shin, J. H. Han, J. Y. Lee, J. App. Surface. Science, **270**, 572 (2013).
[9] C. Guille, J. Herrero, J. Vacuum, **84**, 924 (2010).
[10] Y. Xiaocheng, X. Chunchuan, N. C. GilesIntrinsic, J. App. Phy., **84**, 737271 (2008).
[11] K. Seoungwoo, B. Seokhwan, K. Inhoe et. al, Mat. Sci. Forums, **544**, 689 (2007).
[12] S. W. Shin, J. H. Han, J. Y. Lee, Y. C. Park et.al, J. App. Surface Science, **270**, 572 (2013).
[13] S. L. Shi, S. J. Xu, J. App. Phy., **109**, 53511 (2011).
[14] P. Wu-Dong, Transactions Electrical and Electronic Materials, **13**, 196 (2012).
[15] A. O. Pudov, Impact of Secondary Barriers on $CuIn_{1-x}Ga_xSe_2$ Solar Cell Operation, Thesis Ph.D, Colorado State University, 2005.
[16] M. I. Hossain, C. Puvaneswaran, M. Zaman, M. R. Karim, M. A. Alghoul, N. Amin, Chalcognide Letters, **8**, 315 (2011).